Revista de Chimie
https://revistadechimie.ro
https://doi.org/10.37358/Rev.Chim.1949

Synthesis and Characterization of Water Dispersible Iron Oxide (γ-Fe_2O_3) Nanoparticles for Biomedical Applications

TEODORA MALAERU, DELIA PATROI*, ELENA ENESCU, GABRIELA GEORGESCU, EUGEN MANTA, EROS ALEXANDRU PATROI, VIRGIL MARINESCU, CRISTIAN MORARI, MAGDALENA VALENTINA LUNGU
National Institute for Research and Development in Electrical Engineering ICPE-CA, 313 Splaiul Unirii, Bucharest, 030138, Romania

Abstract: *In this study, L-lysine coated γ-Fe_2O_3 nanoparticles were synthesized by a chemical approach in two steps. In the first step γ-Fe_2O_3 nanoparticles were synthesized by a polyol-reduction method. XRD analysis confirmed the presence of cubic maghemite phase with an average crystallite size of 9.2 nm. SEM analysis showed that the prepared γ-Fe_2O_3 nanoparticles have a spherical structural morphology with the tendency of agglomeration and with size in the range 8.36- 10.69 nm. The γ-Fe_2O_3 nanoparticles were coated with L-lysine in the second stage in an aqueous dispersion with ultrasonication followed by a gentle heating at 40ºC. FT-IR spectroscopy confirmed the presence of L-lysine on the nanoparticles surface and the Zeta potential also supported the coating of nanoparticles with a hydrophilic layer of amino acid (L-lysine) and a good stability in aqueous medium. Hysteresis loop shows a ferromagnetic behavior at room temperature for both samples.*

Keywords*: iron oxide, l-lysine, magnetic nanoparticles, biocompatible, biomedical applications*

1. Introduction

In the last years, sensitive magnetic nanoparticles have found multiples applications in different areas of bioscience, biotechnology, and environmental technologies. In terms of applications in biomedicine, these are based on the use of selected properties such as magnetic separation, magnetic targeting, heat generation, increased MRI contrast [1-3]. For all these applications, magnetic nanoparticles must be stable to oxidation, biocompatible, not agglomerated, and exhibit high magnetization [4]. The most common used magnetic biomaterials are magnetite (Fe_3O_4) and maghemite (γ-Fe_2O_3). Spherical magnetic nanoparticles with a diameter of 5 - 15 nm are ideal particles for most forms of diagnosis or therapy. Iron oxide nanoparticles may have a spherical shape when prepared in solution or in gas. For this reason, in the last period different methods and processes for the preparation of iron oxide nanoparticles have been intensively studied and improved. Many chemical synthesis methods are reported till present for iron oxide nanoparticles preparation: co-precipitation [5-10], thermal decomposition [11, 12], hydrothermal method [13], the solvothermal method [14], the sonochemical method [15, 16], the electrochemical method [17], the microemulsion method [18], and others [19-22]. In order to obtain a magnetically sensitive biocompatible material it is necessary to stabilize the iron oxide nanoparticles either by modifying the surfaces or by incorporating them in biocompatible matrices. The biopolymers used for the modification of magnetic oxide particles must be biocompatible, biodegradable, non-toxic, non-thrombogenic, non-immunogenic and inexpensive. The most used bio-polymers for coating of magnetic oxide particles reported in the literature are: polyethylene glycol (PEG) [23], polyvinyl alcohol (PVA) [24], dextran [25], chitosan [26], polyvinylpyrrolidone (PVP) [27]. Another way to modify the surfaces of magnetic nanoparticles for biomedical applications is by bonding on their surface suitable chemicals that play an important role in the body. Amino acids are part of the desired chemical substances for modifying the surfaces of magnetic nanoparticles.

**email: delia.patroi@icpe-ca.ro*

Of the amino acids, L-lysine plays an important role in the body as a promoter for calcium absorption in the digestive tract, collagen production, is used by several hormones and enzymes and is required for tissue repair [28]. In this study, γ-Fe_2O_3 nanoparticles with surface coated with an amino acid (L-lysine) were prepared in two steps. The γ-Fe_2O_3 nanoparticles were prepared in a first step by a polyol-reduction method. In the second step, the γ-Fe_2O_3 nanoparticles were coated with an amino acid (L-lysine) by an ultrasonication technique. Modifying the surface of γ-Fe_2O_3 nanoparticles with L-lysine ensures the dispersibility, stability in water, and biocompatibility required for diagnosis and targeted drug delivery for cancer therapy.

2. Materials and methods

2.1. Materials

Iron (III) nitrate nonahydrate $Fe(NO_3)_3 \cdot 9H_2O$ (≥98%) purchased from Sigma-Aldrich and Polyvinylpyrrolidone (PVP) (M = 40000 g/mol) from SIGMA were used as reagents. Polyethylene glycol (PEG 200) (99%) purchased from Sigma-Aldrich was used as solvent, Sodium Acetate CH_3COONa (99%) from REACTIVUL was used as a reducing agent, L-lysine as hydrophilic agent for coating from Sigma-Aldrich. Ethylic Alcohol Absolute C_2H_5OH (99.9%) purchased from MERCK and Deionized Ultrapure Water, obtained from a Millipore Simplicity - UV equipment, were used at washing and purification.

2.2. Synthesis of iron oxide (γ-Fe_2O_3) nanoparticles (sample PIb)

An amount of 4.04g of $Fe(NO_3)_3 \cdot 9H_2O$ was dissolved in 50 mL of PEG using magnetic stirring for 30 min. using a 250 mL tree-neck round bottomed flask equipped with condenser, magnetic stirrer, thermometer and heating system. After this stage, it was added 0.375g of PVP as stabilizing agent in the polyol-iron salt solution by magnetic stirring and heating at 100ºC for another 30 min. The obtained solution was subsequently heated up to 240ºC. At this stage it has been added an amount of 4.1015 g of CH_3COONa as reducing agent and it was observed the formation of brown colour precipitate. The reaction solution was refluxed for 4h under these conditions of reaction. The mixture was then cooled down to the room temperature and it was centrifuged in order to remove the PEG and PVP excess traces. Then, the magnetically separated precipitate was washed three times successively with deionized water and absolute ethylic alcohol, and at the end it was dried in a vacuum oven at a temperature of 100°C overnight.

2.3. Synthesis of γ-Fe_2O_3 coated with L-lysine nanoparticles (sample PIIb)

0.22 g of the γ-Fe_2O_3 nanoparticles thus prepared were ultrasonically dispersed in 25 mL of H_2O D.I (Deionized water) for 10 min. Then, 4 mL of 1% L-lysine solution was added to this suspension and has been dispersed ultrasonically for another 30 min. The reaction mixture thus obtained was then heated to 40ºC for 3 h under magnetic stirring. After cooling to room temperature, the nanoparticles were separated from the suspension by magnetic decantation and washed three times with H_2O D.I and finally with absolute ethylic alcohol, then were dried under vacuum at room temperature overnight.

2.4. Characterization

The powders of γ-Fe_2O_3 nanoparticles and γ-Fe_2O_3 nanoparticles coated with L-lysine were analysed by X-ray diffraction (XRD) technique in order to establish the crystalline structure and to evaluate the crystallite size and the lattice parameters. X-ray diffractometry analysis was performed with the D8Discover (Bruker) diffractometer, configured on the primary optics with a primary radiation tube of Cu (λ = 1.540598Å), 0.6 mm Göebel mirror, and on the secondary optics with a 1D LynxEye detector. The diffractograms were recorded with an angular increment of 0.04°, at a scan speed of 1s/step. Qualitative analysis was performed using the ICDD Release 2015 database. Considering the main crystallographic phases, by the Rietveld analysis, the parameters of the elementary cell, respectively the average crystallite size were determined. Fourier Transform Infrared (FT-IR) spectroscope (Perkin Elmer

Spectrum 100) was used to characterize the L-lysine coated γ-Fe_2O_3 nanoparticles. The powder samples were ground with KBr and compressed into a pellet. FT-IR spectra were recorded in range of 4000 - 400 cm^{-1} with a resolution of 4 cm^{-1}. The morphology and particle size of the as prepared samples were investigated by FESEM-FIB (Workstation Auriga) scanning electron microscope equipped with a dispersive X-ray spectroscope (EDS) detector (Oxford Instruments). Elemental compositions were evaluated by energy dispersive X-ray spectroscopy (EDS) area scanning system. The magnetic properties of iron oxide samples were measured with a vibrating - sample magnetometer (VSM) Lake Shore 7300 model at room temperature. The prediction of the dispersion stability and particle size of the γ-Fe_2O_3 coated with L-lysine in aqueous solution was determined using NanoBrook ZetaPlus Zeta Potential Analyzer (Brookhaven, USA).

3. Results and discussions

XRD analysis

The X-ray powder diffraction pattern of the sample (PIb) of γ-Fe_2O_3 nanoparticles processed by a polyol-reduction synthesis method is presented below in Figure 1.

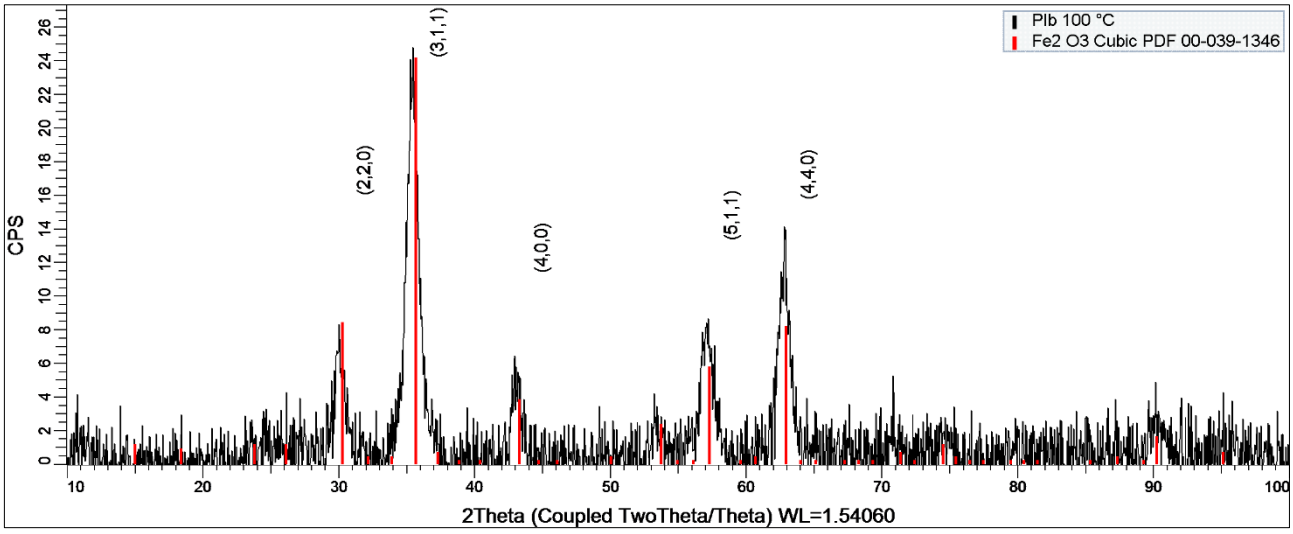

Figure 1. X-ray diffraction patterns of γ-Fe_2O_3 nanoparticles sample prepared by a polyol-reduction method

The peaks can be indexed by the (2 2 0), (3 1 1), (4 0 0), (5 1 1) and (4 0 0) crystalline planes. All the diffraction peaks in the patterns of sample (PIb) matched well with the standard γ-Fe_2O_3 reflection according to the ICDD PDF2 (01-089-5892) data sheet. As it is well known, both structures of magnetite (Fe_3O_4) and maghemite (γ-Fe_2O_3) nanoparticles have same XRD peaks. However, considering that black color is characteristic for magnetite and brown for maghemite, the sample in our experiment is of brown color which supports the successful formation of the maghemite phase. The crystallite size was obtained using Debye-Scherer equation [29] considering the main peak (311). The crystallite size and the main parameters of the as obtained samples determined are presented in Table 1.

FT-IR analysis

FT-IR spectra of sample (PIb) of iron oxide nanoparticles synthesized by polyol-reduction method and of sample (PIIb) of nanoparticles of iron oxide coated with L-lysine are given in Figure 2(a-b).

Table 1. XRD analysis main parameters of the γ-Fe_2O_3 nanoparticles samples

Sample	Crystalline phase	2 Θ (degrees)	d (Å)	hkl	Lattice parameter		Crystallite size (nm)
					a_{theor} (Å)	a_{exp} (Å)	
PIb	γ-Fe_2O_3 - cubic structure; Space group Fd-3mZ	30.077	2.9687	(2,2,0)	8.3457	8.3910	9.2
		35.42	2.5322	(3,1,1)			
		43.032	2.1002	(4,0,0)			
		57.099	1.6117	(5,1,1)			
		62.766	1.4701	(4,4,0)			

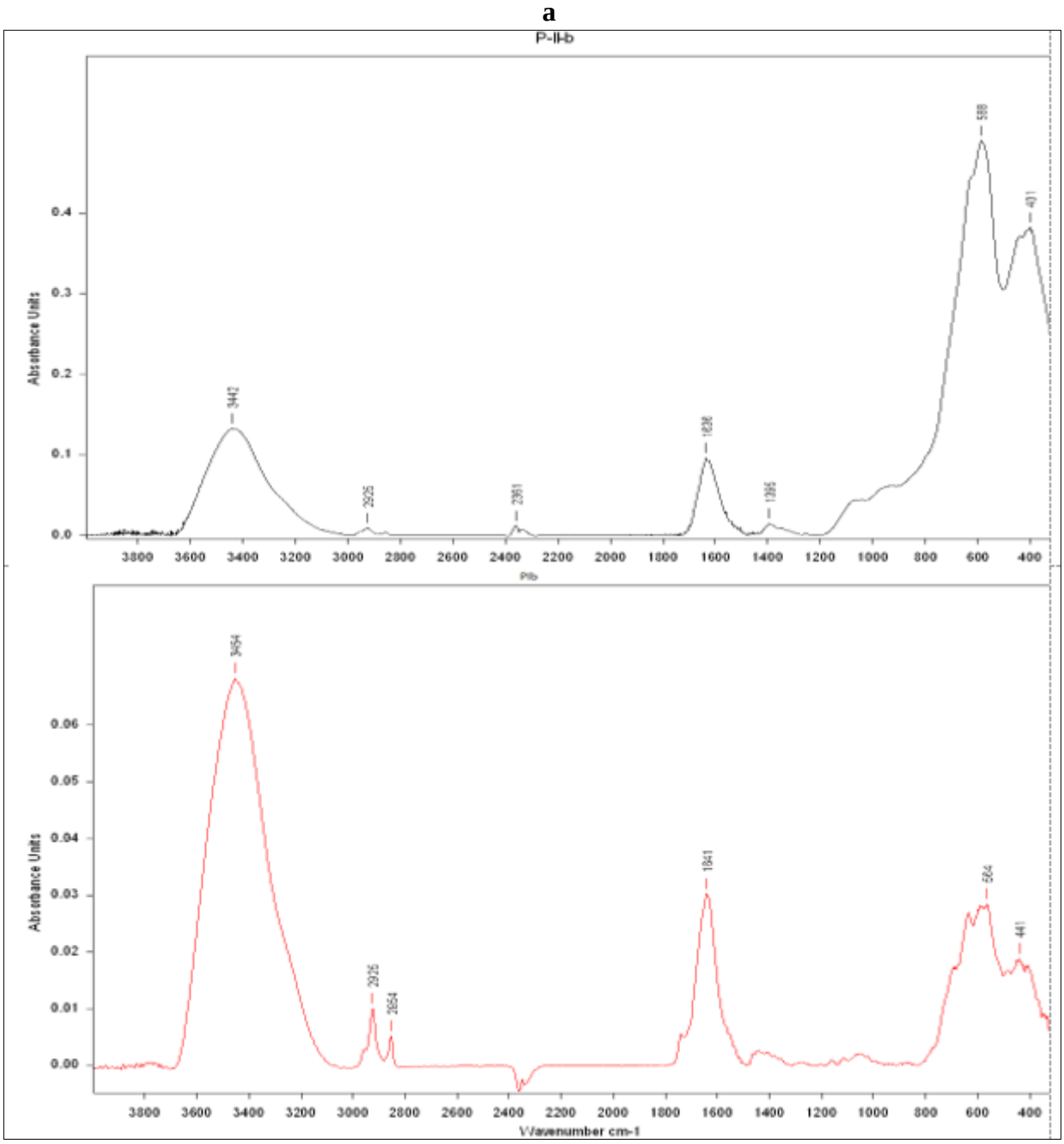

Figure 2. The FT-IR spectra recorded on sample PIb of iron oxide nanoparticles obtained by polyol-reduction synthesis method (a) and on sample PIIb of L-Lysine coated iron oxide nanoparticles (b)

For samples PIb and PIIb, IR spectra exhibits two absorption bands at 441 cm^{-1}, 564 cm^{-1} and respectively at 401 cm^{-1} and 564 cm^{-1}, which are assigned the Fe-O stretching modes corresponding in the maghemite phase [28]. In the spectrum in Figure 2(a) the absorption bands at 3454 cm^{-1} and 1641 cm^{-1} are assigned to O-H stretching and deformation vibration which indicates the presence of hydroxyl groups on the surface of γ-Fe_2O_3 nanoparticles [27]. Also, in this spectrum the presence of two peaks is observed at 2925 cm^{-1} and 2854 cm^{-1} given by the symmetrical and asymmetrical stretching vibrations of the C-H bonds, due to the presence of the stabilizing agent (PVP) on the surface of the nanoparticles. In the spectrum in Figure 2 (b) two peaks are observed at 1636 cm^{-1} and 1391 cm^{-1} assigned to the vibrations of asymmetric and symmetric stretching of carboxyl anion from the structure of L-lysine. The splitting between the asymmetric and symmetric stretching of carboxyl group is higher than 200 cm^{-1} indicating a unidentate coordination between the carboxyl group and the hydroxyl group on the nanoparticles surface [8]. The peak at 2925 cm^{-1} is given by asymmetrical stretching vibration of the C-H bond and peak at 3442 cm^{-1} is assigned to the stretching vibration of N-H bond from the amino acid structure. The absorption peak at 2361 cm^{-1} may be due to the absorption of CO_2 on the surface of nanoparticles. According to these results, FT-IR analysis confirms the coating of γ-Fe_2O_3 nanoparticles thus prepared with L-lysine.

EDS-analysis

By the EDS analysis of the chemical composition of the samples it was evaluated the EDS spectrum of the as synthesized γ-Fe_2O_3 nanoparticles (Figure 3(a)). It was noticed the existence of Fe, O and C elements, the C element being related to the presence of PVP capping agent on the nanoparticle surface, also in agreement with the FT-IR analysis [29]. Further, EDS pattern of the L-lysine coated γ-Fe_2O_3 nanoparticles (Figure 3(b)) evidenced the Fe, O, C elements and in addition the presence of the N element. The result is in agreement with the result of the FT-IR analysis and confirms the presence of the superficial amino acid layer (L-lysine) on the γ-Fe_2O_3 nanoparticles thus prepared.

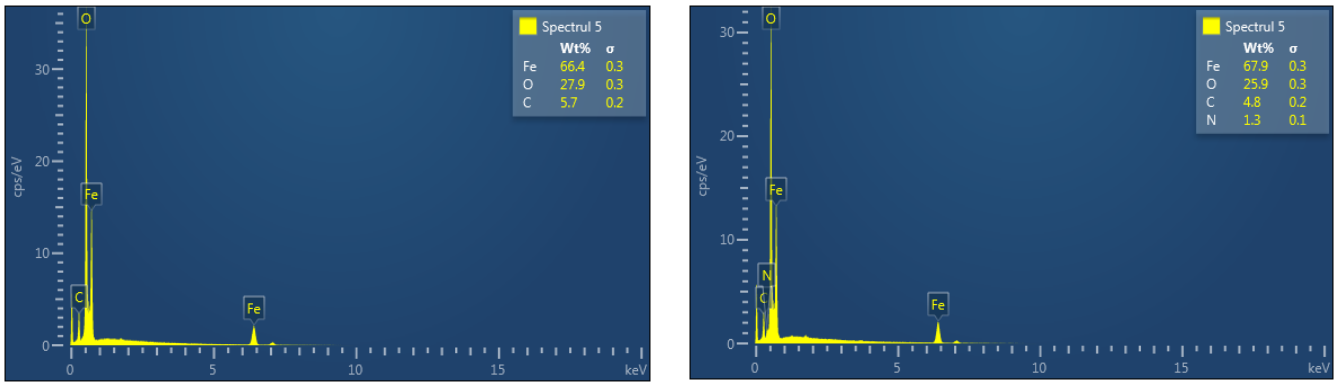

(a) (b)

Figure 3. The EDS pattern of γ-Fe_2O_3 nanoparticles obtained by polyol-reduction synthesis method: (a) nanoparticles not coated with L-lysine and (b) nanoparticles coated with L-lysine

SEM analysis

The morphological scanning electron image of the γ-Fe_2O_3 nanoparticles synthesized by polyol-reduction method is presented in Figure 4.

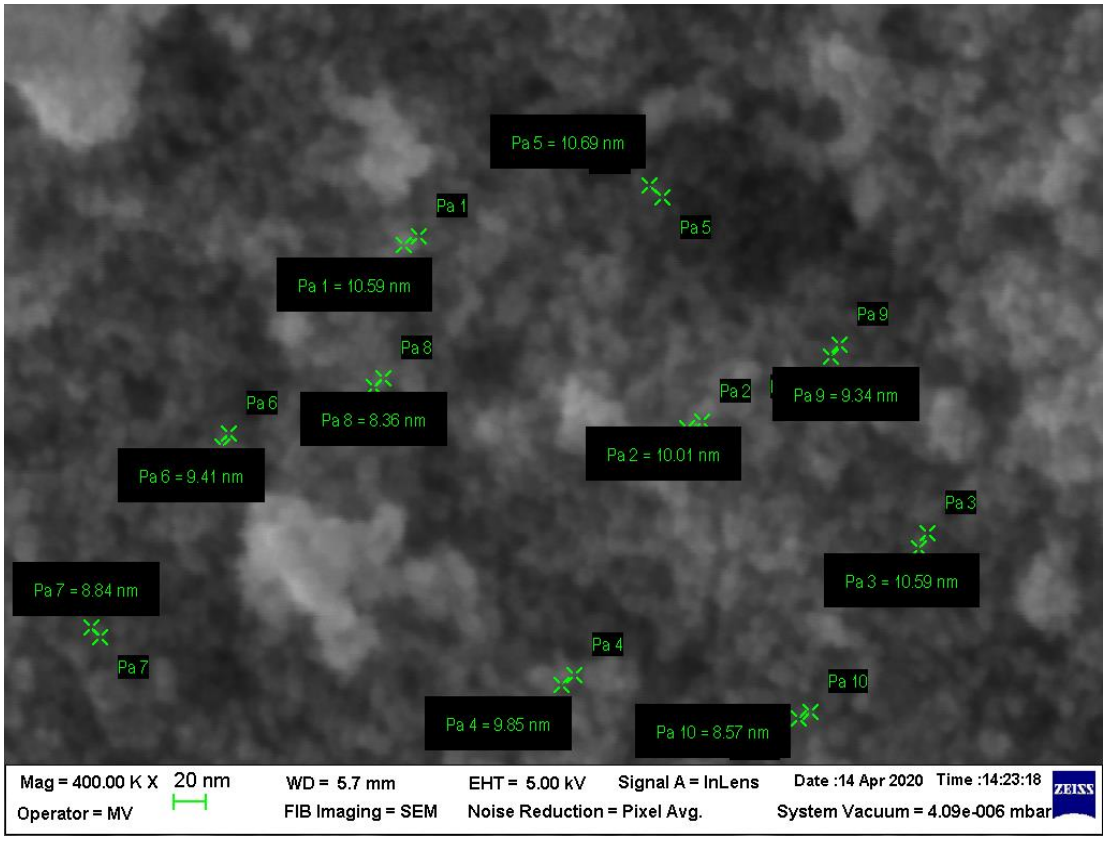

Figure 4. The SEM image of the γ-Fe_2O_3 nanoparticles nanoparticles obtained by polyol-reduction synthesis method (sample PIb)

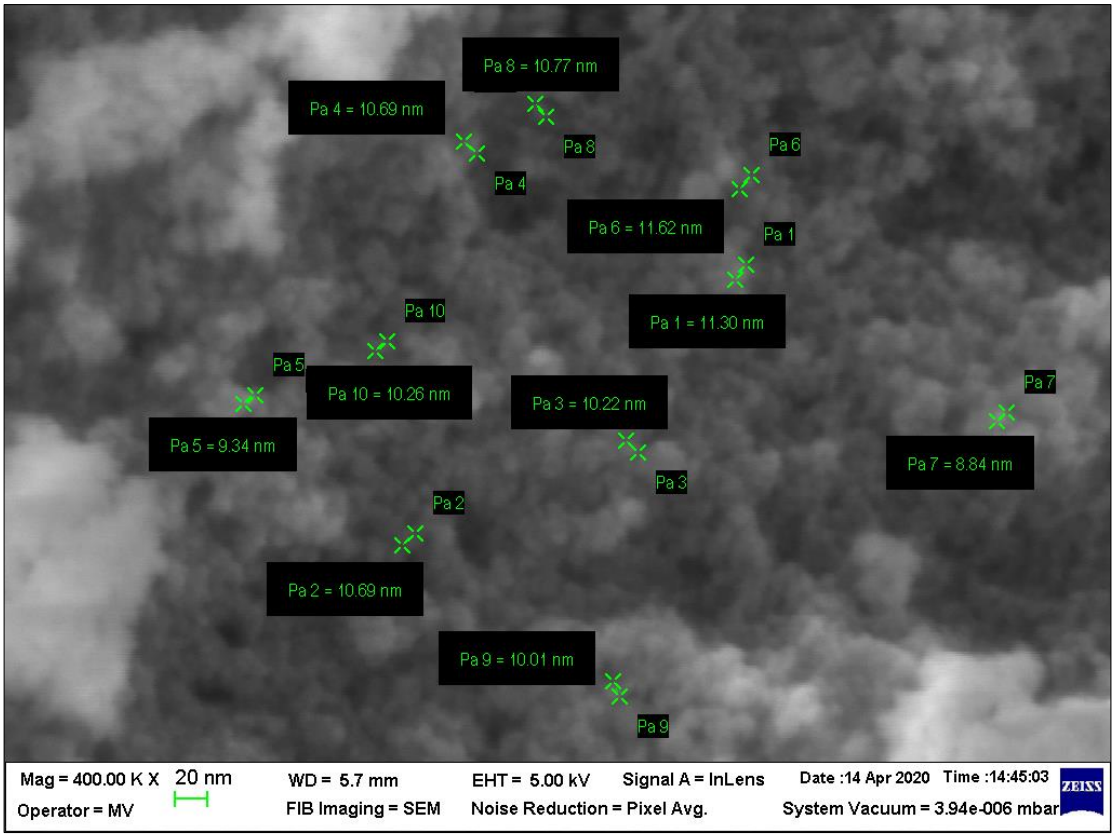

Figure 5. The SEM image of the γ-Fe_2O_3 -L-lysine coated nanoparticles obtained by Polyol-reduction synthesis method (sample PIIb)

The as prepared γ-Fe_2O_3 nanoparticles morphology indicate an approximate spherical shape being noticed also a predisposition to form conglomerates. The size of particles, as evaluated by the SEM analysis, it was in range 8.36 - 10.69 nm. Also the γ-Fe_2O_3 nanoparticles coated with L-lysine (Figure 5) are of spherical shape with size in range 8.84 - 11.62 nm. The increase in nanoparticle size in this case is explained by the presence of the L-lysine layer.

VSM analysis

The magnetic properties of the nanoparticles of γ-Fe_2O_3 and γ-Fe_2O_3 coated with L-lysine were measured at room temperature by vibrating sample magnetometry and hysteresis loops are presented in Figure 6.

The saturation magnetization (M_s), coercive field (H_c) and remanence magnetization (M_r) values are given in Table 2.

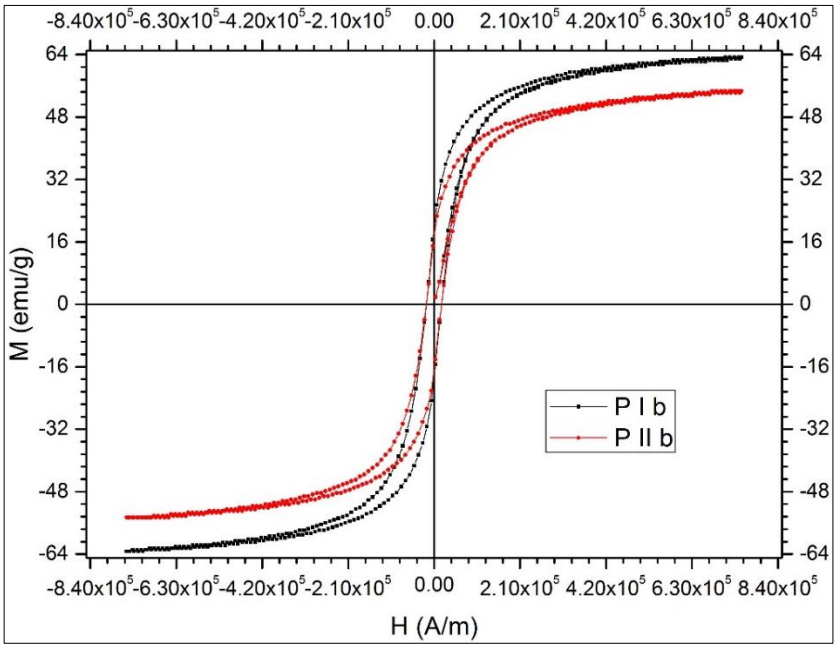

Figure 6. The magnetic hysteresis loops for the γ-Fe_2O_3 obtained by polyol-reduction synthesis method (sample PIb) and for L-lysine coated γ-Fe_2O_3 nanoparticles (sample PIIb)

Table 2. Magnetic parameters of the γ-Fe_2O_3 and γ-Fe_2O_3 coated with l-lysine nanoparticles samples

Sample	Remanent magnetization (M_r) [emu/g]	Saturation magnetization (M_s) [emu/g]	Coercivity field (H_c) [A/m]/[Oe]
PIb	18.80	63.32	18501.76/ 232.5
PIIb	16.96	54.43	18700.70/ 235

From the shape of the hysteresis loops it conclude that the nanoparticles have ferromagnetic behaviour at room temperature.

The saturation magnetization (Ms = 63.32 emu/g) value for the γ-Fe_2O_3 nanoparticles (sample PIb) is lower than that of the bulk γ-Fe_2O_3 (76 emu/g) due to the presence of PVP at surface the nanoparticles and the small size effect of the γ-Fe_2O_3 particles confirmed by the well-known direct dependence between magnetization and the diameter of small particles (diameters smaller than ca.15 nm). The M_s (M_S = 54.43 emu/g) of γ-Fe_2O_3 nanoparticles coated with L-lysine (sample PIIb) decreases due to the diamagnetic amino acid layer on the surface of the nanoparticles and also due to the quantitative reduction of γ-Fe_2O_3

in the sample. Therefore, the γ-Fe_2O_3 nanoparticles coated with L-lysine have magnetic properties characteristic for biomedical applications.

Particle size and zeta potential analysis

Figure 7(a-b) shows dynamic light scattering measurement results for nanoparticles of γ-Fe_2O_3 and γ-Fe_2O_3 coated with L-lysine.

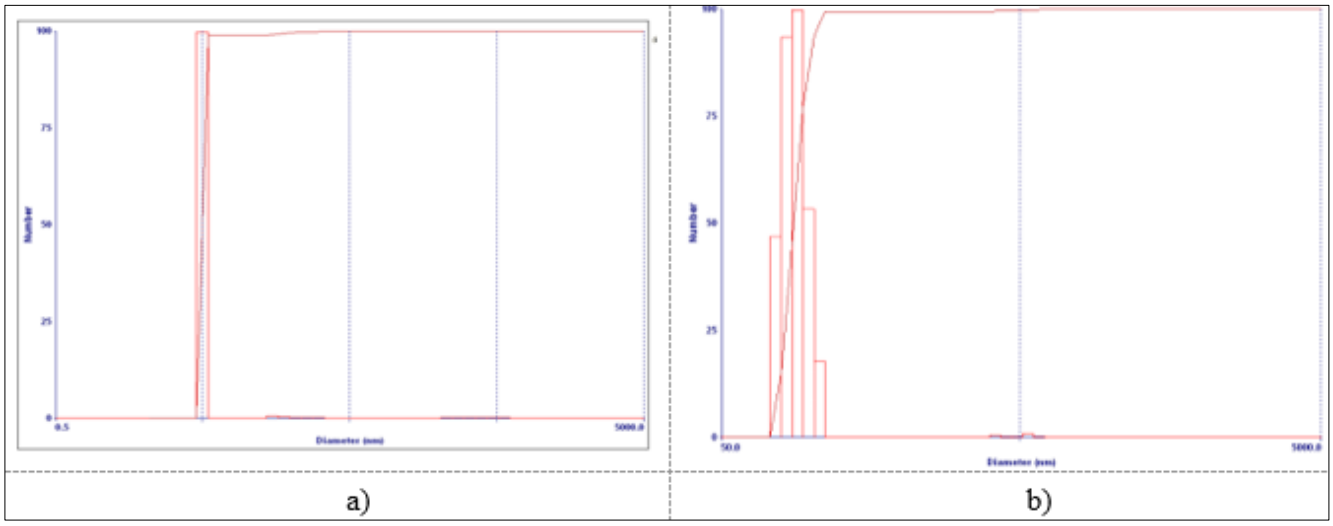

Figure 7. DLS measurement results for: a) γ-Fe_2O_3 nanoparticles and (b) γ-Fe_2O_3 coated with L-lysine

Particles size analysis revealed bimodal distribution of nanoparticles with an effective diameter of 161.3 nm and 0.365 polydispersity index for γ-Fe_2O_3 nanoparticles, and an effective diameter of 270.5 nm with 0.327 polydispersity index for γ-Fe_2O_3 coated with L-lysine nanoparticles. The effective diameter of γ-Fe_2O_3 coated with L-lysine nanoparticles is larger than uncoated γ-Fe_2O_3 nanoparticles, which proves the presence L-lysine layer on their surface. The mean hydrodynamic diameters obtained by DLS method are also larger than those measured by SEM, because DLS measures the aggregated clusters of nanoparticles in aqueous solution. In order to determine the stability of the aqueous dispersion of γ-Fe_2O_3 coated with L-lysine nanoparticles, the Zeta potential was also performed. The values of Zeta potential recorded at different time intervals on an aqueous solution (0.01%) are shown in Figure 8(a–b).

The value of the Zeta potential decreases in time from -35.56 mV (initially) to the value of -33.90 mV (after 1 month). Maintaining the high value of the Zeta potential outside the range of +30 ÷ -30 mV shows a good stability in aqueous medium of γ-Fe_2O_3 coated with L-lysine nanoparticles thus prepared.

a

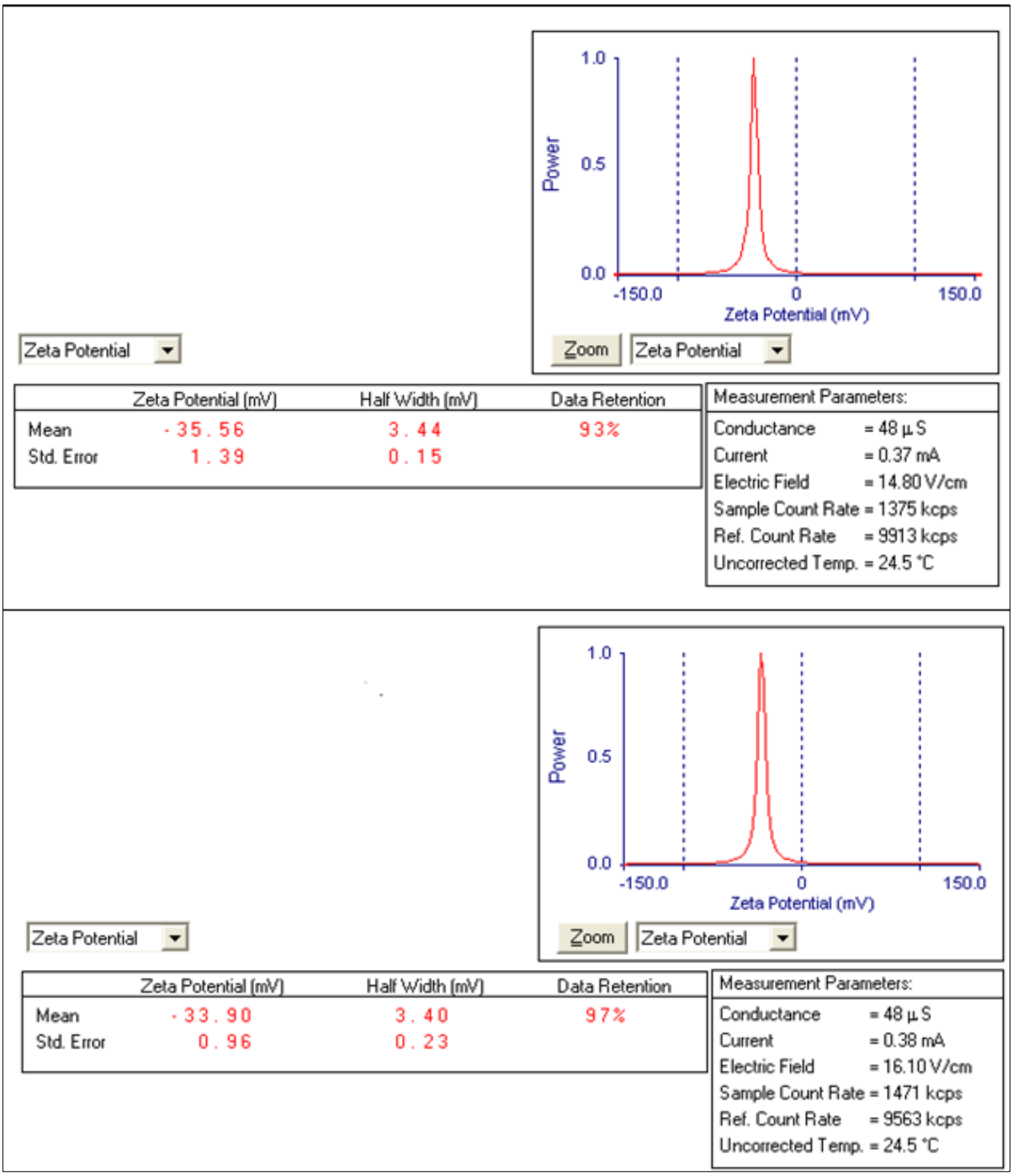

b

Figure 8. The Zeta potential analysis of the γ-Fe_2O_3 coated with L-lysine nanoparticles in aqueous medium: a) initially and b) after 1 month

4. Conclusions

In this study we have developed a facile chemical approach for synthesis of water dispersible iron oxide (γ-Fe_2O_3) nanoparticles in two steps. In the first step were synthesized γ-Fe_2O_3 nanoparticles by a polyol-reduction method. XRD analysis confirmed the unique phase of maghemite with average crystallite of 9.2 nm. The surface coverage of the nanoparticles thus prepared with L-lysine in the second stage was confirmed by FT-IR, EDS and zeta potential analysis. The zeta potential values of -35.56 mV (at baseline) and of -33.90 mV (after time of 1 month) recorded on the aqueous dispersion of γ-Fe_2O_3 nanoparticles coated with L-lysine indicate a good dispersibility in water and stability over time. The

VSM analysis evidenced a ferromagnetic behavior of the nanoparticles at room temperature. The good magnetic properties (M_s = 54.43 emu/g) and good dispersion and stability in the aqueous medium meet the requirements for biomedical applications.

Acknowledgments: This work was finnacialy supported by project PN no. 19310103 (5103)/2019 and project no. 30 PFE/2018 between National R&D Institute for Electrical Engineering ICPE-CA and Romanian Ministry of Education and Research.

References

1. PANKHURST, Q.A., CONNOLLY, J., JONES, S.K., DOBSON, J., Applications of magnetic nanoparticles in biomedicine *J. Phys. D: Appl. Phys*., **36**(13), 2003, 167-181. DOI:10.1088/0022-3727/36/13/201
2. SHALINI, R., CHARLES, U., PITTMAN Jr., DINESH, M., Magnetic magnetite (Fe_3O_4) nanoparticle synthesis and applications for lead (Pb^{2+}) and chromium (Cr^{6+}) removal from water, *J. Colloid. Interface Sci*., **468**, 2016, 334-346. https://doi.org/10.1016/j.jcis.2015.12.008
3. BULTE, J.W., Intracellular Endosomal Magnetic Labeling of Cells, *Methods Mol. Med*., **124:** Magnetic Resonance Imaging, Springer, 2006, 419-439. https://doi.org/10.1385/1-59745-010-3:419
4. BOGUSLAVSKI, Y, MARGEL, S., Synthesis and characterization of poly(divinylbenzene)-coated magnetic iron oxide nanoparticles as precursor for the formation of air-stable carbon-coated iron crystalline nanoparticles, *J. Colloid Interface Sci.*, **317**(1), 2008, 101-114. https://doi.org/10.1016/j.jcis.2007.09.014
5. WU, S., SUN, A.Z., ZHAI, F.Q., WANG, J., XU, W.H., ZHANG, Q., VOLINSKY, A.A., Fe_3O_4 Magnetic Nanoparticles Synthesis from Tailings by Ultrasonic Chemical Co-precipitation, *Mater. Lett*., **65**(12), 2011, 1882-1884. https://doi.org/10.1016/j.matlet.2011.03.065
6. SALAVATI-NIASARI, M., MAHMOUDI, T., AMIRI, O., Easy Synthesis of Magnetite Nanocrystals via Coprecipitation Method, *J. Cluster Sci*., **23**, 2012, 597-602. https://doi.org/10.1007/s10876-012-0451-5
7. COVALIU, C.I., GEORGESCU, G., JITARU, I., NEAMTU, J., MALAERU, T., OPREA, O., PATROI, E., Synthesis and Characterization of a Hydroxyapatite Coated Magnetite for Potential Cancer Treatment, *Rev. Chim*, **60**(12), 2009, 1254-1257
8. MALAERU, T., PATROI, E.A., MARINESCU, V., OPREA, O., PATROI, D., MORARI, C., MANTA, E., GEORGESCU, G., Preparation and Characterization of Fe_3O_4 Magnetic Nanofluid in Vegetable Oil, *Rev. Chim*, **70**(2), 2019, 459-464
9. UNSOY, G., GUNDUZ, U., OPREA, O., FICAI, D., SONMEZ, M., RADULESCU, M., ALEXIE, M., FICAI, A., Magnetite: From Synthesis to Applications, *Curr. Top. Med. Chem*., **15**(16), 2015, 1622-1640. DOI: 10.2174/1568026615666150414153928
10. ZHANG, L., HUANG, Z., SHAO, H., LI, Y., ZHENG, H., Effects of γ-Fe_2O_3 on γ-Fe_2O_3/Fe_3O_4 composite magnetic fluid by low-temperature low-vacuum oxidation method, *Materials & Design*, **105**, 2016, 234-239. https://doi.org/10.1016/j.matdes.2016.05.077
11. AMARA, D., GRINBLAT, J., MARGEL, S., Solventless thermal decomposition of ferrocene as a new approach for one-step synthesis of magnetite nanocubes and nanospheres, *J. Mater. Chem*., **22**, 2012, 2188-2195. https://doi.org/10.1039/C1JM13942H
12. ASUHA, S., ZHAO, S., WU, H.Y., SONG, L., TEGUS, O., One step synthesis of maghemite nanoparticles by direct thermal decomposition of Fe–urea complex and their properties, *J. Alloys. Compd*., **472**, 2009, L23-L25. https://doi.org/10.1016/j.jallcom.2008.05.028
13. YOU, L-J, XU, S., MA, W-F, LI, D., ZHANG, Y-T, GUO, J., HU, J.J., WANG, C-C., Ultrafast Hydrothermal Synthesis of High Quality Magnetic Core Phenol–Formaldehyde Shell Composite Microspheres Using the Microwave Method, *Langmuir*, **28**(28), 2012, 10565-10572. https://doi.org/10.1021/la3023562

14. TIAN, Y., YU, B., Li, X., Li, K., Facile solvothermal synthesis of monodisperse Fe_3O_4 nanocrystals with precise size control of one nanometre as potential MRI contrast agents, *J. Mater. Chem.*, **21**, 2011, 2476-2481. https://doi.org/10.1039/C0JM02913K
15. ZHU, S., GUO, J., DONG, J., CUI, Z., LU, T., ZHU, C., ZHANE, D., MA, J., Sonochemical fabrication of Fe_3O_4 nanoparticles on reduced graphene oxide for biosensors, *Ultrason, Sonochem*, **20**(3), 2013, 873-880. https://doi.org/10.1016/j.ultsonch.2012.12.001
16. ZHANG, S., ZHANG, Y., WANG, Y., LIU, S., DENG, Y., Sonochemical formation of iron oxide nanoparticles in ionic liquids for magnetic liquid marble, *Phys. Chem. Chem. Phys*., **14**(15), 2012, 5132-5138. https://doi.org/10.1039/C2CP23675C
17. RAMIMOGHADAM, D., BAGHERI, S., HAMID, S.B.A., Progress in electrochemical synthesis of magnetic iron oxide nanoparticles, *J. Magn. Magn. Mater*., **368**, 2014, 207-229. https://doi.org/10.1016/j.jmmm.2014.05.015
18. WONGWAILIKHIT, K., HORWONGSAKUL, S., The preparation of iron (III) oxide nanoparticles using W/O microemulsion, *Mater. Lett*., **65**(17), 2011, 2820-2822. https://doi.org/10.1016/j.matlet.2011.05.063
19. LI, J.; MENGUY, N., GATEL, C., BOUREAU, V., SNOECK, E.; PATRISRCHE, G.; LEROY, E.; PAN, Y., Crystal growth of bullet-shaped magnetite in magnetotactic bacteria of the Nitrospirae phylum, *J R Soc. Interface*, **12**(103), 2015, 20141288. DOI: 10.1098/rsif.2014.1288
20. LEMINE, O. M., OMRI, K, ZHANG, B., EL MIR, L., SAJIEDDINE, M., ALYAMANI., A., BOUOUDINA, M., *Superlattices Microstruct*, **52**(4), 2012, 793-799. DOI:10.1016/j.spmi.2012.07.009
21. PANDEY, S., MISHRA, S., Sol-gel derived organic-inorganic hybrid materials: Synthesis, characterizations and applications, *J. Sol-Gel Sci. Technol*., **59**(1), 2012, 73-94. DOI:10.1007/s10971-011-2465-0
22. RUHUL, A.B., PALASH, B., BIRINCHI, K. DAS, Controlled synthesis of α- and γ-Fe_2O_3 nanoparticles via thermolysis of PVA gels and studies on α-Fe_2O_3 catalyzed styrene epoxidation, *J. Saudi Chem. Soc*., **21**(1), 2017, S170-S178. https://doi.org/10.1016/j.jscs.2013.12.010
23. BUNKER, A., Poly(Ethylene Glycol) in Drug Delivery, Why Does it Work, and Can We do Better? All Atom Molecular Dynamics Simulation Provides Some Answers, *Phys. Procedia*, **34**(3), 2012, 24-33. https://doi.org/10.1016/j.phpro.2012.05.004
24. MOHAN, L., VERMA, S.R., Synthesis and Characterization of Poly Vinyl Alcohol Functionalized Iron Oxide Nanoparticles, *Macromol. Symp*., **376**, 2017, 1-5. https://doi.org/10.1002/masy.201700017
25. CAN, H.K., KAVLAK, S., PARVIZIKHOSROSHAHI, S., GÜNER, A., Preparation, characterization and dynamical mechanical properties of dextran-coated ironoxide nanoparticles (DIONPs), *Artif. Cells Nanomed. Biotechnol*., **46**(2), 2018, 421-431. https://doi.org/10.1080/21691401.2017.1315428
26. QU, J., LIU, G., WANG, Y., HONG, R., Preparation of Fe_3O_4-chitosan nanoparticles used for hyperthermia, *Adv. Powder Technol*., **21**(4), 2010, 461-467. DOI:10.1016/j.apt.2010.01.008
27. ISA K., MUSTAFA, A., MOHAMMAD, R. G., PARVIZ, N., SIMINDOKHT, S-A., TAHER, D., PEIR, H.K., A novel method for preparation of bare and poly(vinylpyrrolidone) coated superparamagnetic iron oxide nanoparticles for biomedical applications, *Mater. Lett*., **179,** 2016, 5-8. https://doi.org/10.1016/j.matlet.2016.05.048
28. DURMUS, Z., KAVAS, H., TOPRAK, M. S., BAYKAL, A., ALTINÇEKIÇ, T. G., ASLAN, A., BOZKURT, A., COȘGUN, S., L-lysine coated iron oxide nanoparticles: Synthesis, structural and conductivity characterization, *J. Alloys Compd*, **484**, 2009, 371-376. https://doi.org/10.1016/j.jallcom.2009.04.103
29. MALAERU, T., ENESCU, E., GEORGESCU, G., PATROI, D., EUGEN MANTA, E., PATROI, E.A., MORARI, C., MARINESCU, V., Synthesis and Characterization of Hydrophilic γ-Fe_2O_3 Nanoparticles for Biomedical Applications, *Rev. Chim*., **70**(6), 2019, 2026-2031.

Manuscript received: 8.05.2020